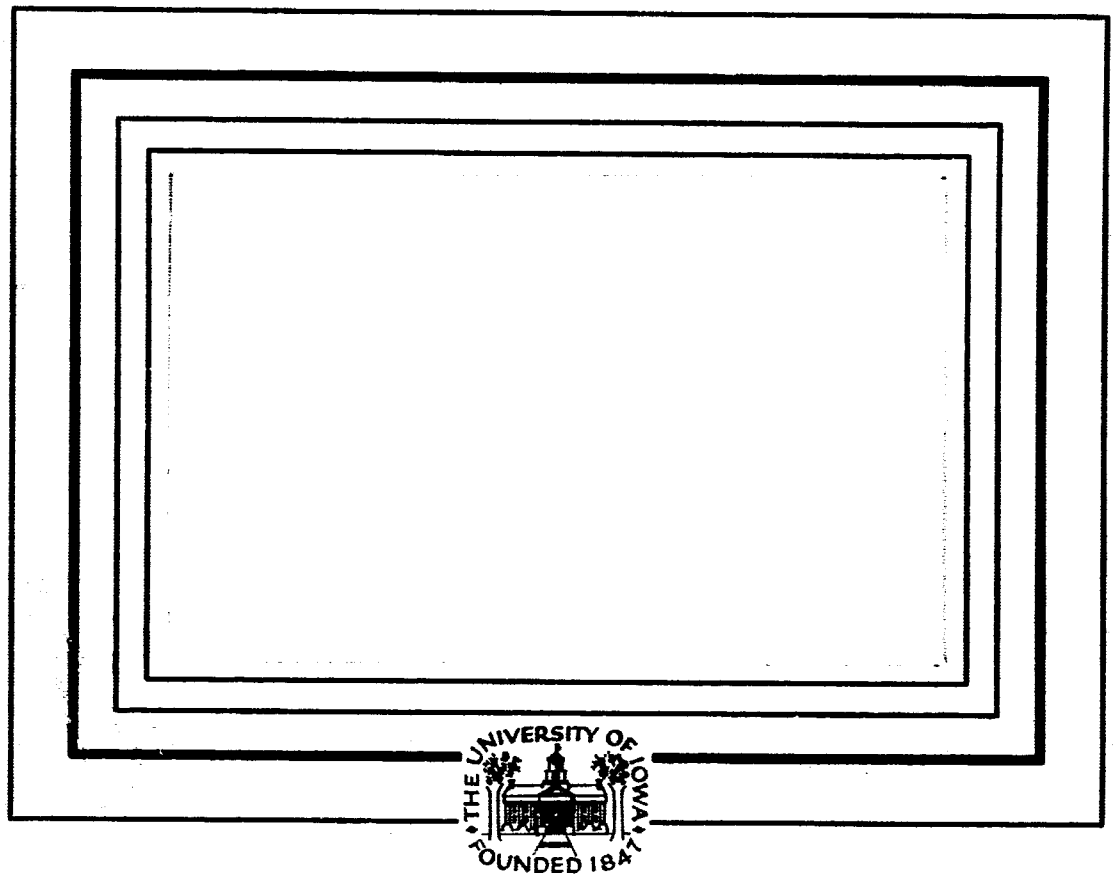

Department of Physics and Astronomy
THE UNIVERSITY OF IOWA
Iowa City, Iowa

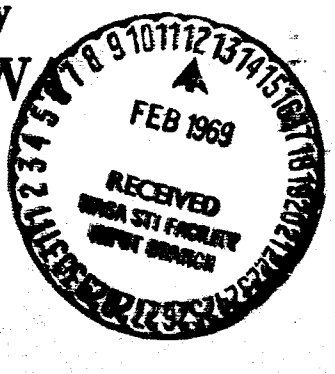

U. of Iowa 69-3

Solar X-Ray Control of the E Layer of the Ionosphere*

by

P. R. Sengupta**

Department of Physics and Astronomy
University of Iowa
Iowa City, Iowa 52240

January 1969

*Research supported in part by the National Aeronautics and Space Administration under grant (NsG 233-62.) NGL-16-001-002

**Now at Indian Institute of Technology, Department of Electronics, P.O. Kharagpur, Dt. Midnapore, West Bengal, India.

ABSTRACT

Solar X-ray control of the E layer of the ionosphere is investigated. Electron production rates between 100 and 140 km above the earth due to 31-100 A° solar X-ray flux extrapolated from X-ray data recorded by N.R.L. experiments on Explorer 30, OGO-4, and OSO-4, and due to reported Lyman alpha flux from rocket and satellite experiments are calculated to show that about 70% of the E-layer ionization is contributed by the X rays. Calculated E-layer electron densities due to solar X-ray flux on two typical days are compared with the E-layer electron density profile. $f_oE/\cos\chi$ over Ottawa (45° N) and Washington, D. C. (39° N) during November 1966 to March 1967 are seen to be closely related with 44-60 A° X-ray flux measured by the N.R.L. detector on Explorer 30. Correlation with 8-20 A° flux is poorer. $(f_oE)^4/\cos\chi$ over Manila (15° N) and Breisach (48° N) during the period July 1966 to June 1968 exhibits a linear relation with X-ray flux. The relation is given approximately by:

$$(f_oE)^4/\cos\chi = a + b \cdot F(31\text{-}100\ A°) + c \cdot F(10\text{-}30\ A°) .$$

The first term represents ionization due to XUV and is related to the 11-year sunspot cycle. The second and the third terms represent X-ray contribution and show day-to-day variation depending on the daily solar activity level, in addition to the 11-year variation with sunspot cycle.

Effective recombination coefficients of the layer calculated from the term coefficients are in agreement with accepted values.

It is concluded that 31-100 A° solar X rays which contribute about 70% of the E-layer ionization on a day of moderate solar activity are responsible for day-to-day variations in the E-layer index. Contribution of 10-30 A° solar flux to the E-layer ionization is small except on a day of high solar activity.

I. INTRODUCTION

According to contemporary theory E-layer formation is due to the following ionization processes:

(1) Ionization of molecular oxygen and molecular nitrogen by 10-100 A° X rays;

(2) Ionization of molecular oxygen by XUV-radiation in the Lyman β line (1025.7 A°) and by Lyman continuum (865-912 A°); and

(3) Atomic oxygen ionized by XUV-radiation in Lyman continuum and by X rays.

The problem of relative importance of these processes is not yet resolved.

In this paper we have evaluated the relative importance of X-ray and ultraviolet ionization from a correlation between f_oE, the ordinary ray critical frequency of the E layer, and integrated solar X-ray flux in 8-20 A° and 44-60 A° bands recorded by N.R.L. detectors on Explorer 30, OGO-4, and OSO-4 satellites. The daily average of solar flux in these bands is reported in I.E.R., solar geophysical data bulletin published from ESSA, Boulder, by the U. S. Department of Commerce. f_oE data used in the present analysis were supplied by Ionospheric Tele-Communication Laboratory, ESSA, Boulder, and Air Force Cambridge Research Laboratories,

Massachusetts. XUV data are taken from published papers by Neupert [1964] and Hinteregger et al. [1966].

Results of the present analysis show that about 70% of the E-layer ionization is due to 30-100 A° X rays. Day-to-day variation of the E-layer indices is traced to the relative importance of X-ray ionization.

II. INSTRUMENTATION

Explorer 30 satellite was launched on 18 November 1965 by a NASA Scout vehicle from the NASA station at Wallops Island, Virginia. The orbital elements of the satellite are: apogee altitude, 899 km; perigee altitude, 691 km; and inclination, 58°. The satellite transmits the recorded solar X-ray and UV data in real time by means of an FM/AM telemetry system operating on a frequency of 136.530 Mc/s. In order to provide continuity of 44-60 A° and 8-16 A° X-ray monitoring during those periods when the satellite is out of range of the NASA STANDAN network, a storage system has been included which samples the output from each of these photometers once every five minutes. The stored data are transmitted to the ground station by a separate digital transmitter.

The system of X-ray detectors consist of six photometers and four G.M. counters with different window thicknesses. The bands covered are 0.5-3, 1-8, 8-20, 0-20, and 44-60 A°. The G.M. counters cover the 0.5-3 A° and 1-8 A° regions. In Table I all the information pertinent to the 1-20 A°, 8-16 A°, and 44-60 A° detectors is presented, while the wavelength response curves are shown in Figs. 1a and 1b. Table I contains the angular positions equivalent to the letter positions designated in the figures.

An aspect system, included in the instrumentation, measures the aspect angle between the satellite equatorial plane and the satellite-sun direction. The angular response of all photometers has been measured and correction for the aspect angle is obtained from these measurements. The satellite produces useful data during periods of good aspect which is about 300 days in a year. For the rest of the time the aspect angle is too large to allow reasonable corrections [Kreplin, 1966].

Grey body spectrum is assumed for reducing signals to flux values with $T_g = 0.5 \times 10^6$ °K for 44-60 A° range and $T_g = 2 \times 10^6$ °K for 8-20 A° and 0-8 A° ranges. The current flux conversion factor for each photometer and each wavelength band has been calculated. These conversion factors are given in Table II [Kreplin, 1966]. Explorer 33 (1965-93A) ceased to function on 12 November 1967. Naval Research Laboratory's X-ray monitoring experiments on NASA's OGO-4 and OSO-4 satellites are the sources of data from November 1967. The detectors on these satellites are similar to those on Explorer 30 and the method of data reduction is also similar [Descriptive Text, Solar Geophysical Data, February 1968].

III. DATA AND ANALYSIS

Explorer 30 X-ray data published monthly in I.E.R. solar geophysical data bulletin consist of tables of observing times and daily averages of solar X-ray flux. Outstanding events are also listed. The table combines the data reported by the N.R.L. Laboratory; ESSA, Boulder; and Aberdeen, South Dakota.

X-ray and ionospheric data for nearly two years from June 1966 to March 1968 are used in the present analysis. Midday values of the E-layer indices are considered. Weekly and monthly averages of both X-ray and ionospheric data are computed in order to eliminate scatter due to probable observational errors. f_oE values over Manila (15°N), Washington, D. C. (38°N), Ottawa (45°N), and Briesach (48°N) have been used in the present study. These stations are chosen to include both low latitude and mid-latitude stations. Doubtful or uncertain observations and flare events are excluded from the averages.

Weekly and monthly averages of X-ray flux are obtained from published daily averages. It is now known that 21-100 A° solar flux remains nearly constant over a period of about 24 hours except during a flare. Daily average, therefore, is a fairly reliable approximation for the midday flux. This approximation, however, is less reliable for

10-20 A°, flux. However, non-flare 10-20 A° flux is small compared to 21-100 A° flux. Hence relative importance of non-flare 10-20 A° contribution to E layer is small. For computing X-ray flux average only those days are included for which f_oE average is computed.

In Figs. 2 and 3 weekly averages of midday f_oE over Washington, D. C. are plotted together with weekly averages of F(8-20 A°) cosχ and F(44-60 A°) cosχ for November 1966, January 1967, and February 1967, χ being the midday solar zenith angle for the corresponding week. Similar plots for Ottawa are shown in Figs. 4 and 5. Correlation with 44-60 A° flux is more than 90% for both the stations. Correlation with 8-20 A° is poorer.

In Figs. 6 and 7 monthly averages of $(f_oE)^4/\cos\chi$ over Manila and Breisach are plotted against monthly averages of F(44-60 A°) for the period July 1966 to March 1968. A linear relationship between the two quantities is clearly evident. The scatter may be attributed to:

(1) Experimental Error. At low flux values calibration uncertainty is relatively large. Error in f_oE measurement is of greater consequence because the quantity appears in the fourth power.

(2) Change in XUV Contribution Due to Change in XUV Flux. 1968 XIV flux value would be higher than 1966 value because of sunspot maximum in 1969.

The positive intercept on the X axis gives the mean XUV contribution. The value of this intercept is $\simeq$ 80 units in both the figures. The slopes are also equal being $\simeq$ 60 units per 0.1 erg of 44-60 A° flux, 44-60 A° flux is about 33% of the total 31-100 A° flux. This gives a slope of $\simeq$ 200 units per erg of 31-100 A° flux. The dotted line in Fig. 6 corresponds to the upper limit while those in Fig. 7 correspond to lower and upper limit of XUV contribution.

Figures 8 and 9 show the relation between F(8-20 A°) and $(f_oE)^5/\cos\chi$ over the same stations for the same period. There are fewer points in these two figures than in Figs. 5 and 6 due to lack of useful F(8-20 A°) data. One interesting point clearly evident in Figs. 7 and 8 is that E-layer index is independent of F(8-20 A°) for flux values less than 10^{-2} erg/cm^2 sec. It will be shown later than ionization due to X-ray flux less than 10^{-2} erg/cm^2 sec is small compared to E-layer ionization. For higher values of F(8-20 A°), $(f_oE)^4/\cos\chi$ is linearly proportional to the flux. The slope for both the stations is $\simeq$ 22 units per 0.1 erg of flux. 10-30 A° flux is about 1.2 times the 8-20 A° flux. Hence the slope is 18 units per 0.1 erg of 10-30 A° flux. This value is slightly lower than that for 31-100 A° flux.

IV. THEORY

Ionization processes in the E region are:

(1) Molecular oxygen ionized by 10-100 A° X rays and by ultraviolet radiation of Lyman β type and also by the Lyman continuum at $\lambda < 910$ A°;

(2) Molecular nitrogen ionized only by 10-100 A° X rays; and

(3) Atomic oxygen ionized by ultraviolet radiation of the Lyman continuum at $\lambda \leq 910$ A° and by X rays.

The unit optical depth for the 10-100 A° spectral range is concentrated in the layer about 20 km thick centered near 105 km. But due to K absorption edge of nitrogen and oxygen (see Figs. 10 and 11) two spectral ranges must be considered, viz., 10-30 A° and 31-100 A°. Both these ranges have comparable absorption cross-sections. The photoionization for each atomic or molecular constituent may be calculated from the equation

$$q_i(h) = \int_0^{\lambda_i} \eta_i (\lambda)\, \sigma i (\lambda)\, Ni (h)\, \varphi(\lambda, h)\, d\lambda \qquad (1)$$

[Van Zandt and Knecht, 1964]

where q_i, σi, and Ni are the ionization rate, absorption cross section

and particle density respectively of the ith constituent; φ is the radiation flux at height h of wavelength λ, λi is the longest wavelength at which photoionization of ith constituent occurs and ηi the ionization efficiency (ion pairs/photon absorbed). The total rate of electron production at height h is given by

$$q(h) = \sum_i q_i (h) \tag{2}$$

Solar radiation flux φ at the height h is related to the flux φ_o above the earth's atmosphere by the equation

$$\varphi (\lambda, h) = \varphi_o (\lambda) e^{-\tau (\lambda, h)} \tag{3}$$

The optical depth τ is given by

$$\tau(\lambda,h) = \sec \chi \Sigma \sigma i \int_h^\infty Ni(h)\, dh \tag{4}$$

For a plane wave of monochromatic ionizing radiation of wavelength λ_o, Eq. (1) may be written in the familiar Chapman form:

$$q(h, \lambda_o, \chi) = \Phi_o \lambda_o \cos\chi \ \eta_{(\lambda o)} \frac{\tau_o(h)}{Ho} \exp [-\tau_o(h)] \tag{5}$$

where

$$N(h) = \sum_i (Ni(h) = N(h_o) \exp\left[- \frac{h-ho}{Ho}\right] ,$$

and Ho is the scale height assumed to be constant above h_o. τ_o in Eq. (5) corresponds to average effective optical depth.

Total electron production rate is obtained by adding the contributions due to radiation of all wavelengths above the ionization threshold, i.e.,

$$q(h, \chi) = \sum_{\lambda_o=\lambda_1}^{\lambda_2} q(h, \lambda_o, \chi) \qquad (6)$$

N(h) and Ni(h) profiles which depend on solar activity are available from the atmospheric models compiled from rocket data for different solar activity levels. σi's are available from laboratory measurements. Figures 10 and 11 show the values of σi used in the present work. CIRA [1965] mean atmospheric model is used for Ni(h). Knowing the radiation flux ionization rate at different heights can be calculated using Eqs. (1) and (2) or (5) and (6). As the satellite measurements give integrated flux over different bands it is necessary to know the spectral energy distribution within the band for computing q.

Grey-body spectral energy distribution is assumed for solar X-ray emission with $T_g = 2 \times 10^6$ °K for 8 - 20 A°, and T_g - 0.5 $\times 10^6$ °K for 21 - 100 A° range.

Results of the computations are given in Figs. 12 through 15. Figure 12 shows the computed molecular oxygen and nitrogen ion production rate per unit energy flux in each of 31-40 A°, 41-60 A°, and 61-100 A° bands for overhead sun. X-ray ionization of atomic oxygen is small compared to ionization of molecular oxygen and nitrogen.

Figure 13 shows the computed total ion production rate by 1.0 erg/cm^2 sec flux in 31-100 A° range together with contribution due to 31-40 A°, 41-60 A°, and 61-100 A° bands. Computed ion production rates due to 10-100 A° flux on 6 April 1967 and due to 1963 value of XUV flux [Hinteregger and Hall, 1966] are plotted in Fig. 14.

Figure 15 shows the computed electron density due to 31-100 A° flux on two typical days together with midday E-layer electron density in the month of April over White Sands, New Mexico, after R. W. Knetch [Ionospheric Radio Propagation, Davis, 1965].

f_oE is related to Ne, the electron density of the layer by the equation

$$(f_oE)^2 = 81\ Ne \qquad (7)$$

where f_oE is given in kc/s and Ne in number per c.c.

The continuity equation for E layer may be written as

$$\frac{dNe}{dt} = q - \alpha_e Ne^2 \tag{8}$$

where α_e is the effective recombination coefficient of the layer. In equilibrium condition we have,

$$q = \alpha_e Ne^2 = \frac{\alpha_e (f_o E)^4}{6.56 \times 10^3} \tag{9}$$

Since q is proportional to cos χ, we have

$$q_o = \frac{\alpha_e (f_o E)^4}{6.56 \times 10^3 \cos \chi} \tag{10}$$

or

$$\alpha_e = \frac{q_o \times 6.5 \times 10^3 \cos \chi}{(f_o E)^4} \tag{11}$$

where q_o is electron production rate for $\chi = 0$. Since q_o is proportional to the radiation flux and is calculated by making use of Eqs. (1) and (2) or (5) and (6), α_e can be calculated if the ratio of radiation flux to the corresponding $(f_o E)^4/\cos \chi$ is known.

V. RESULTS AND DISCUSSION

Combining the results from Figs. 6 to 9 it is possible to arrive at the following relationship:

$$(f_oE)^4/\cos\chi = a + b\,F(31\text{-}100\ A^\circ) + c\,F(10\text{-}30\ A^\circ). \quad (12)$$

Since $(f_oE)^4$ is proportional to the rate of ion production (see Eq. 10), Eq. (12) gives a quantitative measure of the relative importance of X-ray and XUV contribution to E layer ionization. The first term on the right hand side represents contribution due to XUV, the second term represents 31-100 A° contribution, and the third term 10-30 A° contribution. Average values of a, b, and c calculated for six-month periods by solving simultaneous equations with different sets of monthly values during the period are given in Table III. a has the unit of $(Mc/sec)^4$ while b and c are expressed in units of $(Mc/sec)^4/erg\ cm^{-2}\ sec^{-1}$. The value of a which gives the XUV contribution is seen to increase by a factor of 2 from July 1966 to June 1968. This indicates that the XUV flux should have increased by the same factor during the period XUV flux is known to be related to average sunspot numbers. In Fig. 16 half yearly average values of a are plotted together with the half-yearly average of sunspot numbers. There is a close agreement

between the two. For 1963 value of solar XUV flux recorded by rocket and satellite experiments [Hinteregger and Hall, 1966], computed maximum ion production rate at E-layer height is 1.6×10^3 ions per c.c. per sec (see Fig. 14). The 1967 value would be close to the 1963 value because of the sunspot minimum in 1965. Using this value of q_o and substituting the 1967 January-June value of a for $(f_oE)^4/\cos \chi$ in Eq. (11) one obtains

$$\alpha_e = 1.0 \times 10^{-7} \text{ cm}^3 \text{ sec}^{-1} .$$

The second term in Eq. (12) contributes the major part of E-layer ionization. 31-100 A° flux which shows day-to-day variation depending on daily solar activity level, in addition to 11-year variation with sunspot cycle, was found to lie between 0.4 and 1.4 erg/cm^2 sec during the period under study. The minimum value of the flux thus caused 50% of E-layer ionization and the maximum value caused more than 80% of the ionization. Hence, on a day of moderate solar activity 31-100 A° X rays would contribute about 70% of the E-layer ionization. This is in agreement with the computed results shown in Fig. 14. From Fig. 13 maximum rate of ion production at E-layer height due to 1 erg of 31-100 A° X rays is 9×10^3. Using this value for q_o and substituting the value of b for $(f_oE)^4/\cos \chi$ in Eq. (11), one obtains

$$\alpha_e = 3 \times 10^{-7} .$$

Contribution due to the third term is small because 10-30 A° flux which is highly sensitive to solar activity is usually small compared to 31-100 A° flux. Daily average of 10-30 A° flux varied from 1.2×10^{-3} to 8×10^{-2} erg/cm^2 sec during the period under study. For the maximum value of the flux its contribution to E layer ionization was about 20% of the XUV contribution and less than 10% of the total E-layer ionization. The minimum value of the flux (1.2×10^{-2} erg/cm^2 sec) contributed less than 1% of the total ionization.

It is interesting to note that c, the coefficient of the third term, is lower than b, the coefficient of the second term. This means that at E-layer height 31-100 A° X rays are more efficient ionizing agent that 10-30 A° X rays. This is so because 31-100 A° X rays lose almost all their energy between 95 and 115 km altitude, but a part of 10-30 A° flux leaks below 95 km altitude due to K absorption edge of nitrogen and oxygen molecules (see Figs. 9 and 10). The third coefficient c yields a value of $\alpha_e = 3 \times 10^{-7}$. It is significant that both the X ray terms in Eq. (12) yield the same value of α_e while the XUV term yields a lower value of α_e. X rays ionize mainly molecular oxygen and nitrogen, the yield from nitrogen being higher than that from oxygen. XUV on the other hand ionizes atomic and molecular oxygen.

Recent laboratory observations of the dissociative recombination coefficient of the constituents indicate

$\alpha_D(N_2) = (2.8 \pm 5) \times 10^{-7}$ cm^3/sec — Biondi [1964]

$\alpha_D(O_2) = (2.0 \pm 5) \times 10^{-7}$ cm^3/sec — Biondi [1964]

$\alpha_D(NO) = 3.2 \times 10^{-7}$ cm^3/sec — Doering and Mahan [1962]

These values are in good agreement with the α_e calculated from the X-ray term in Eq. (12).

VI. CONCLUSION

From the results discussed above it is possible to make the following conclusions:

(1) 31-100 A° X rays contribute about 50% of the total E-layer ionization on a day of low solar activity, 70% of the ionization on a day of moderate activity, and more than 80% of the ionization on a day of high solar activity.

(2) The response of the E layer to the day-to-day solar activity level may be traced to the relative importance of X-ray ionization.

(3) The variation of E-layer ionization over a sunspot cycle may be traced partly to variation in XUV flux but mainly to the variation of 31-100 A° flux, which varies by a factor of more than 5 from solar minimum to solar maximum.

(4) Contribution of 10-30 A° flux to E-layer ionization is small except on a day of high solar activity or near solar maxima.

(5) Effective recombination coefficient for X-ray ionization agrees with the experimental values of dissociative recombination of the molecular ions.

ACKNOWLEDGEMENTS

The author is grateful to Prof. J. A. Van Allen for providing the necessary facilities for work, and to Dr. R. W. Kreplin of Naval Research Laboratories for making available necessary information about N. R. L. X-ray detectors on Explorer 30. foE data are supplied by Mrs. Dorothy Krop of the World Data Center, ESSA, Boulder and Mr. R. J. Cormier of AFCRL, Hanscomb Field, Massachusetts.

TABLE I

Explorer 30 X-Ray Detectors

Experiment	Position	Window	Thickness(1)	Fill-Gas	Pressure(2)	Effective Window Area(3)
1-20 A°	A	Mylar Aluminum	6.3×10^{-4} 1500A	Carbon Tetrachloride	27	0.10
44-60 A°	B	Mylar	6.3×10^{-4}	Nitrogen	170	0.88
8-16 A°	E	Aluminum	8.9×10^{-4}	Nitrogen	400	0.50
8-16 A°	K	Aluminum	8.9×10^{-4}	Nitrogen	400	1.92

(1) Nominal thickness in cm except where indicated
(2) Pressure in mm Hg at 0°C
(3) cm^2, Attenuation Factor has been included in calculation of effective window area

[Courtesy R. W. Kreplin]

TABLE II

Summary of Current - Flux Conversion Factors for Explorer 30 Experiment

X-ray band & Temp.	8-12A°°	8-20A°	0-20A°			44-60A°
Photometer	2×10^6	2×10^6	10×10^6	2×10^6	0.5×10^6	0.5×10^6
8-16 A° (2) E	2.70×10^9	1.03×10^{10}				
8-16 A° (2) K	7.09×10^8	2.70×10^9				
1-20 A° (2) A				5.14×10^{10}	1.50×10^{10}	
44-60 A° (2)			4.10×10^9	5.57×10^9	6.56×10^7	3.53×10^{10}

(1) Units are °K.

(2) Units for Ion Chamber conversion factors are ergs/$cm^2 sec^{-1} amp^{-1}$.

[Courtesy of R. W. Kreplin]

TABLE III

Period	a	b	c
July - Dec. 1966	55	200	180
Jan. - June 1967	68	205	175
July Dec. 1967	78	200	185
Jan. - June 1968	100	190	170

REFERENCES

Biondi, M. A., Ann. Geophys. 20, 5 (1964).

CIRA - 1965, Compiled by working group IV of the Committee on Space Research (North Holland Publishing Co., 1965).

Davis, K., Ionospheric Radio propagation, Nat. Bur. Standard. Monograph 80 (1965).

Doering, J. P., and B. H. Mahan, J. Chem. Phys. 36, 669 (1962).

Friedman, H., Proceedings of the International Conference on the Ionosphere, 1962, (The Institute of Physics and Physical Society, London, 1963), p. 3.

Hinteregger, H.E., L. A. Hall and S. Schmidtke, Space Research, Vol. VI (MacMillan Co., New York, 1966), p. 1175.

Hinteregger, H.E., and K. Watanbe, J. Geophys. Res. 67, 3373 (1962).

Isthomin, V. G., Artificial Earth Satellites 7, 64 (1961).

Johnson, C. Y., E. B. Meadows and J. C. Holmes, J. Geophys. Res. 63, 443 (1958).

Kreplin, R. W., Private Communication, E. O. Hulburt Center for Space Research, U. S. Naval Research Laboratory, 1965-93 A.

Neupert, W. M., The Physics of Solar Flare, NASA 49, 1963.

Nicolet, M., Electron Density Profiles in Ionosphere and Exosphere, (New York: The MacMillan Co., 1962), p. 116.

Noci, G., and D. Russo, Space Research, Vol. IV (North Holland Publishing Co., Amsterdam, 1964), p. 517.

Norton, R. B., T. E. Van Zandt, and J. S. Denison, Proceedings of the International Conference on the Ionosphere, 1962, (Institute of Physics and the Physical Society, London, 1963), p. 26.

Sengupta, P. R., Trans. Am. Geophys. Union, 49, 253

Sengupta, P. R., X-Ray Emissions from the Quiescent Sun, U. of Iowa 68-12.

Van Zandt, T. E., and R. W. Knecht, Space Physics (John Wiley and Sons, Inc., 1964), p. 166.

Watanbe, K., and H. E. Hinteregger, J. Geophys. Res. 67, 999 (1962).

Whitten, R. C. and I. G. Poppoff, Physics of the Lower Ionosphere, (Prentice Hall, Inc., 1965).

FIGURE CAPTIONS

Figure 1a. Response of 1-20 A° and 44-60 A° photometers on Explorer 30 [courtesy of R. W. Kreplin].

Figure 1b. Response of 8-20 A° photometer on Explorer 30 [courtesy of R. W. Kreplin].

Figure 2. Weekly averages of mid-day f_oE and 8-20 A° flux over Washington, D. C. for November 1966, January and February, 1967.

Figure 3. Weekly averages of mid-day f_oE and 44-60 A° flux over Washington, D. C. for November 1966, January and February 1967.

Figure 4. Weekly averages of mid-day f_oE and 8-20 A° flux over Ottawa for November 1966, January and February 1967.

Figure 5. Weekly averages of mid-day f_oE and 44-60 A° flux over Ottawa for November 1966, January and February 1967.

Figure 6. Relation between monthly averages of $(f_oE)^4/\cos\chi$ and 44-60 A° flux over Manila (15°N) during the period July 1966 to March 1968.

Figure 7. Relation between monthly averages of $(f_oE)^4/\cos\chi$ and 44-60 A° flux over Breisach (48°N) during the period July 1966 to March 1968.

Figure 8. Relation between monthly averages of $(f_oE)^4/\cos\chi$ and 8-20 A° flux over Manila during the period July 1966 to March 1968.

Figure 9. Relation between monthly averages of $(f_0E)^4/\cos\chi$ and 8-20 A° flux over Breisach during the period July 1966 to March 1968.

Figure 10. σ for molecular and atomic oxygen.

Figure 11. σ for molecular nitrogen.

Figure 12. Computed molecular oxygen and nitrogen ion production rate per unit energy flux in 31-40 A°, 41-60 A°, and 61-100 A° bands for overhead sun.

Figure 13. Computed total ion production rate by 1.0 erg/cm^2 sec flux in 31-100 A° range together with contributions due to 31-40 A°, 41-60 A°, and 61-100 A° bands.

Figure 14. Computed ion production rates due to 10-100 A° flux on 6 April 1967 and 1963 value of XUV flux.

Figure 15. Computed electron densities due to 31-100 A° flux on two typical days together with mid-day E layer electron density in April over White Sands (after R. W. Knetch).

Figure 16. Half-yearly average value of 'a' together with half-yearly average of sunspot numbers.

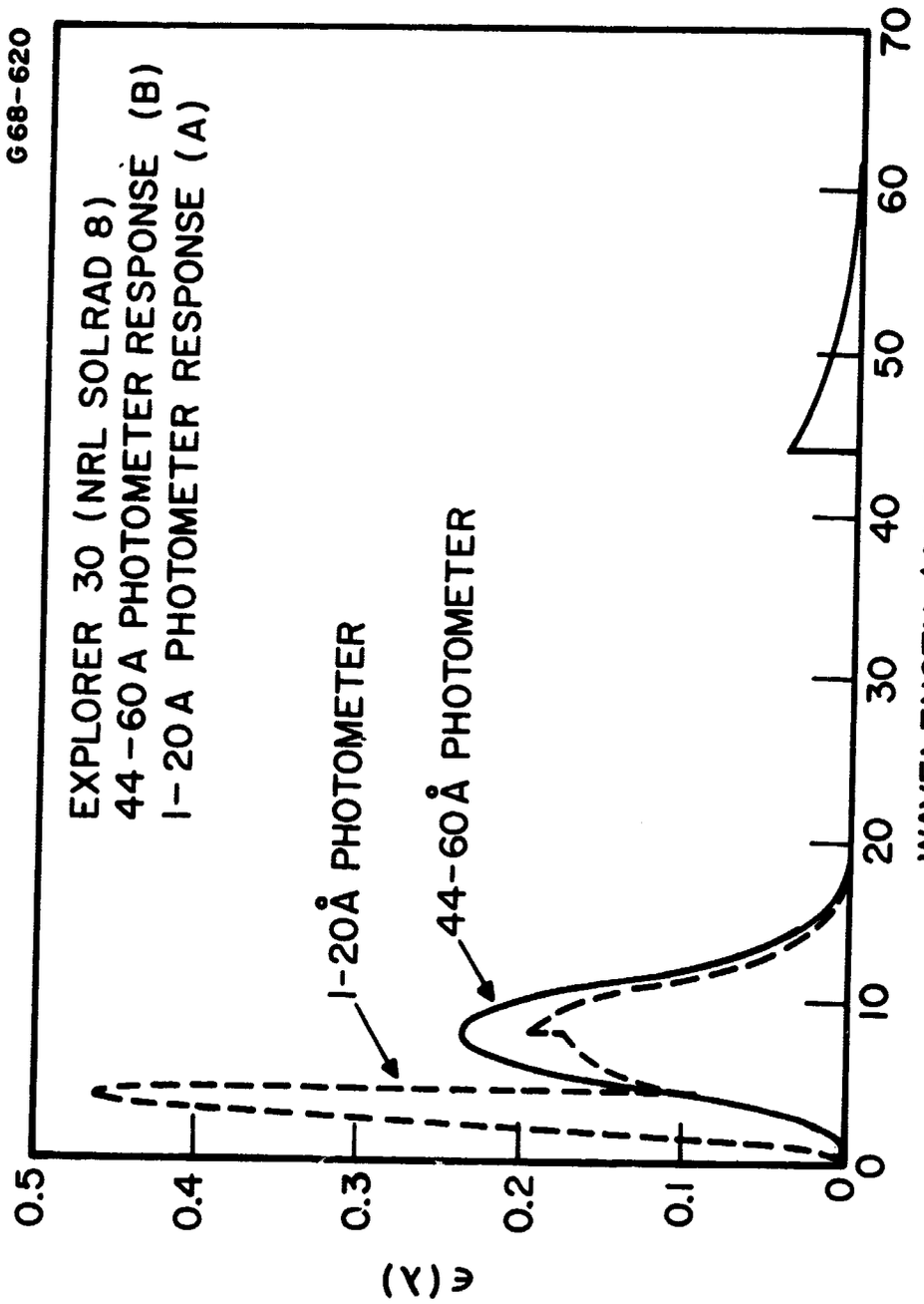
G68-620
EXPLORER 30 (NRL SOLRAD 8)
44-60 A PHOTOMETER RESPONSE (B)
1-20 A PHOTOMETER RESPONSE (A)
1-20Å PHOTOMETER
44-60Å PHOTOMETER
ε(λ)
0.5
0.4
0.3
0.2
0.1
0
0
10
20
30
40
50
60
70
WAVELENGTH (ANGSTROMS)

FIGURE 1a

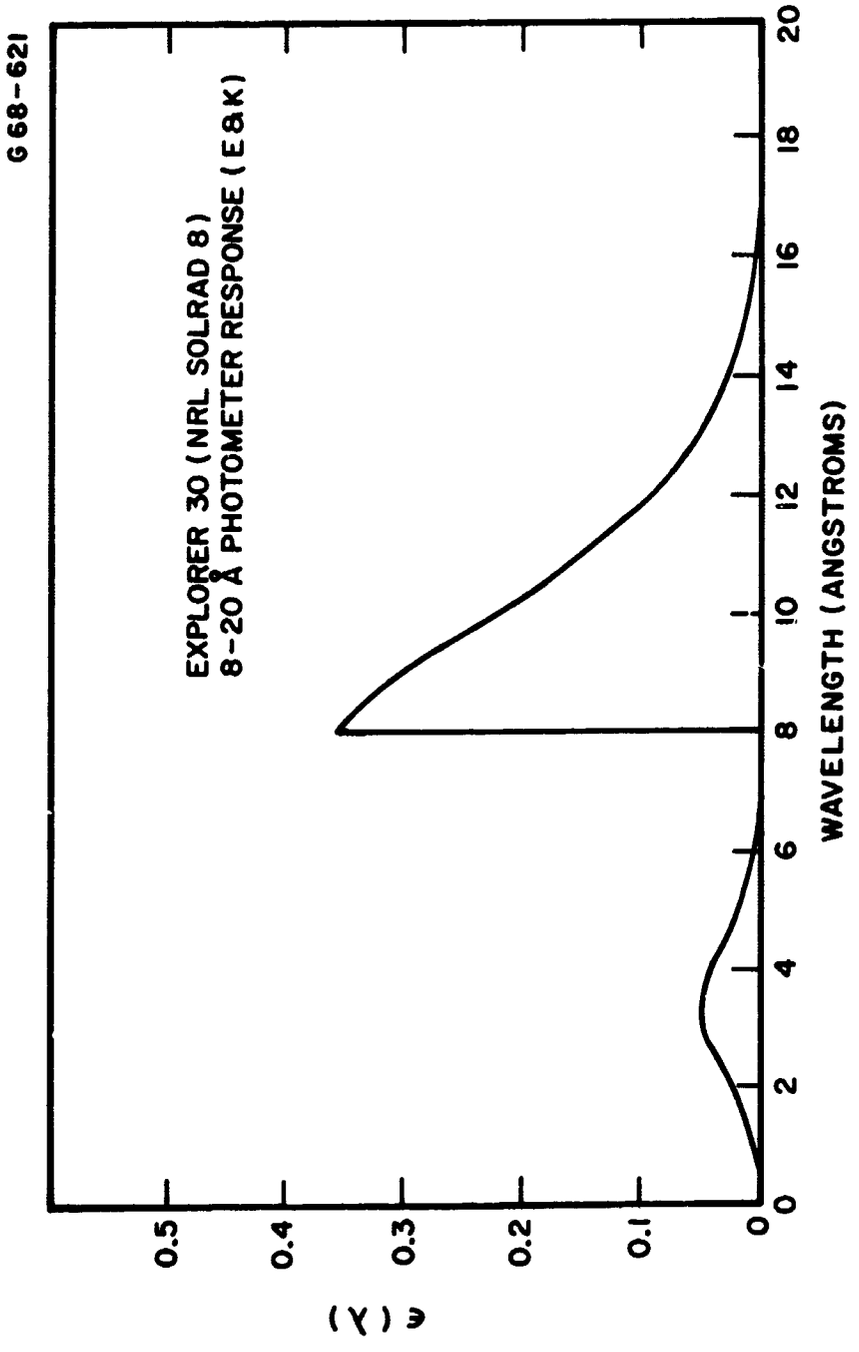
G 68-621
EXPLORER 30 (NRL SOLRAD 8)
8-20 Å PHOTOMETER RESPONSE (E & K)
ε (λ)
0.5
0.4
0.3
0.2
0.1
0
2
4
6
8
10
12
14
16
18
20
WAVELENGTH (ANGSTROMS)

FIGURE I-b

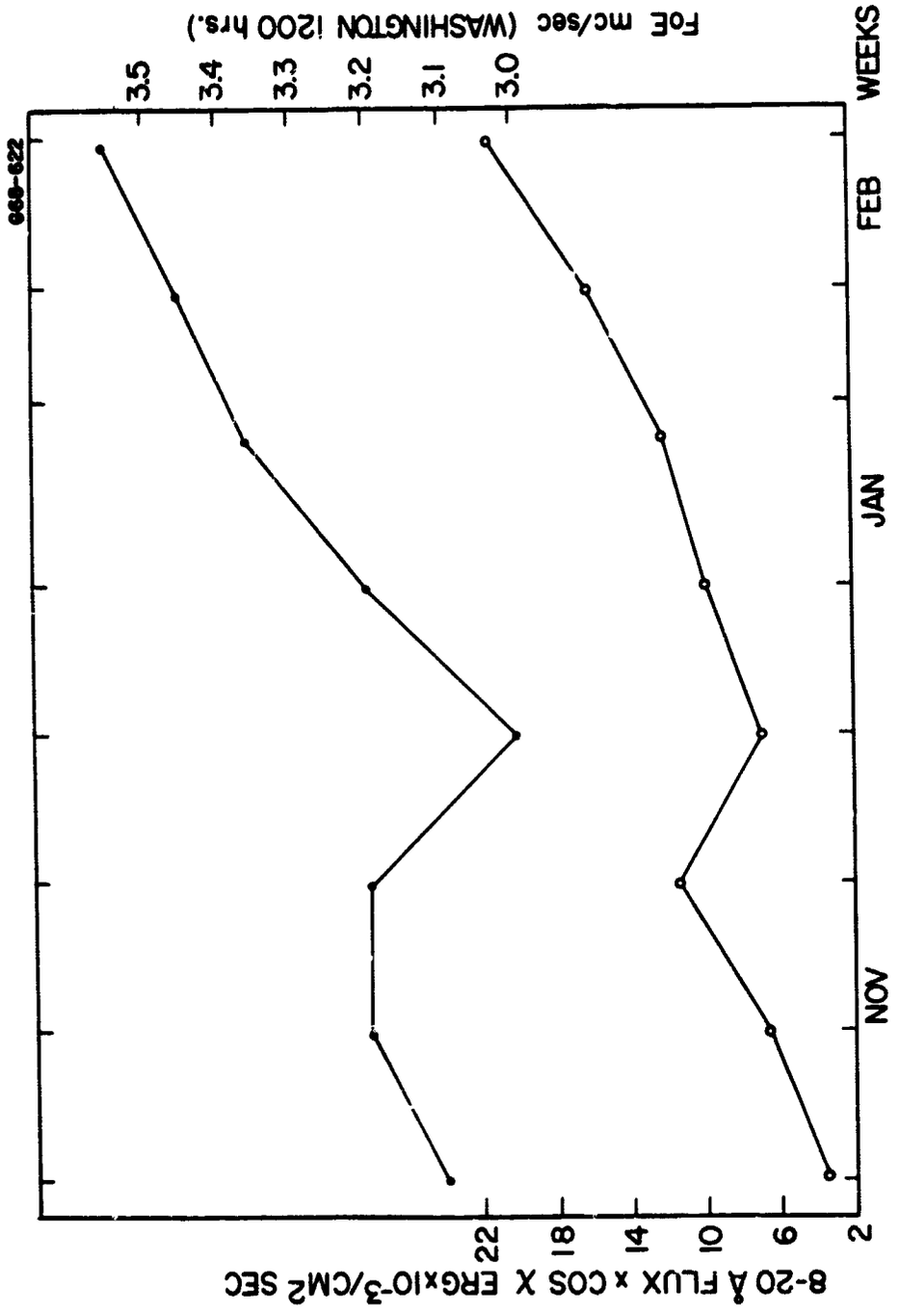
8-20 Å FLUX x COS X ERG×10⁻³/CM² SEC
2
6
10
14
18
22
NOV
JAN
FEB
WEEKS
FoE mc/sec (WASHINGTON 1200 hrs.)
3.0
3.1
3.2
3.3
3.4
3.5
668-622

FIGURE-2

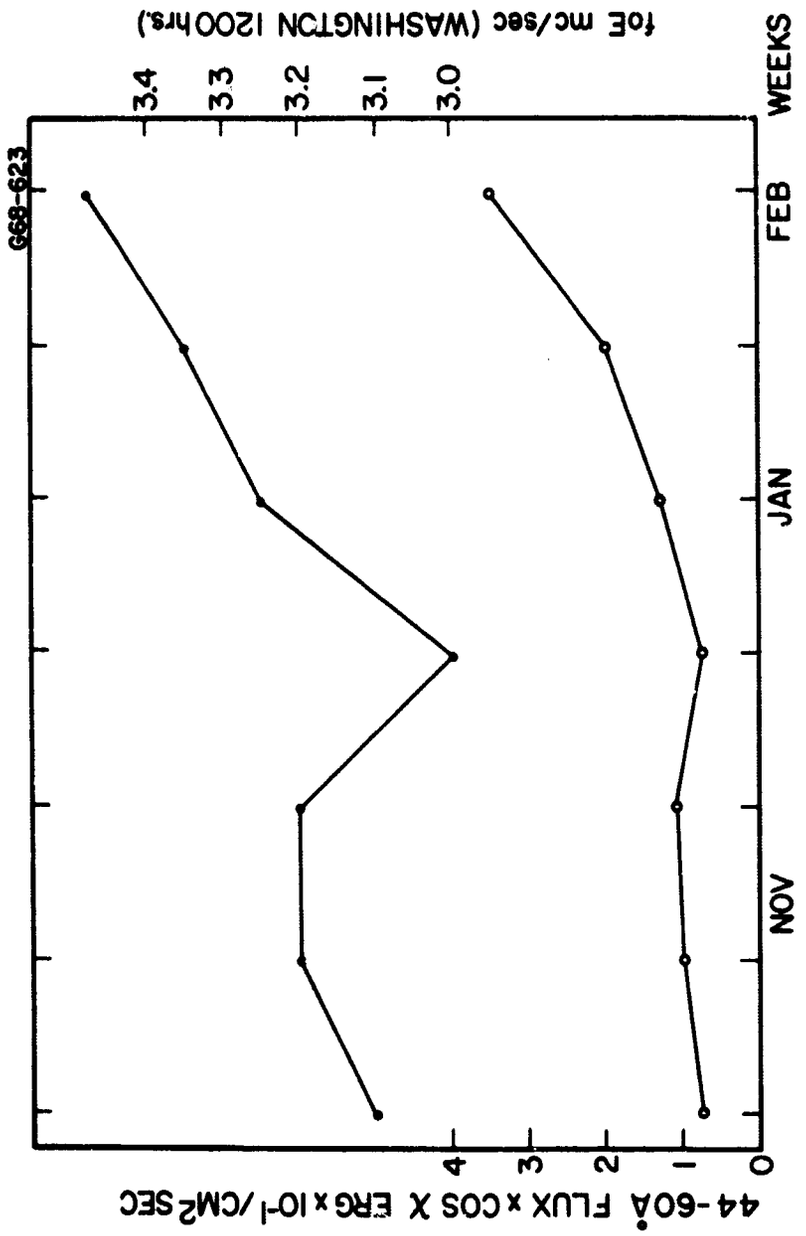
G68-623
NOV
JAN
FEB
WEEKS
0
1
2
3
4
44-60Å FLUX x COS X ERG x 10⁻¹/CM²SEC
3.0
3.1
3.2
3.3
3.4
foE mc/sec (WASHINGTON 1200hrs.)

FIGURE-3

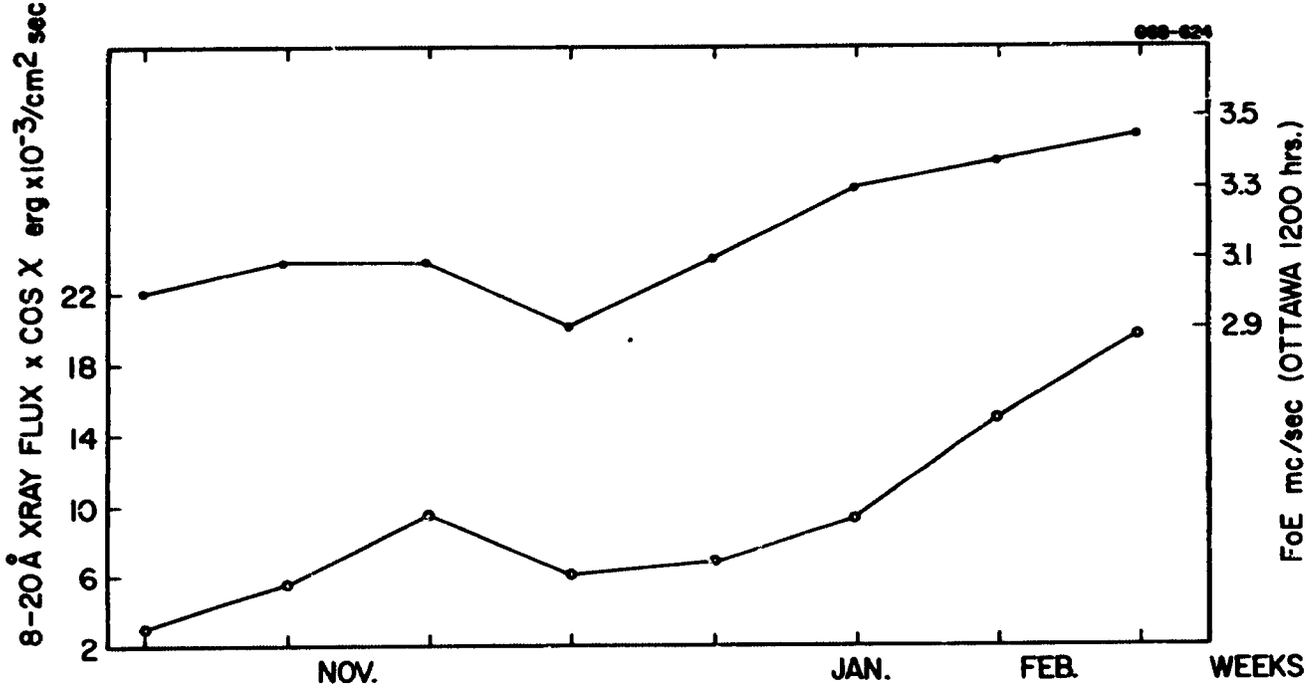
8-20 Å XRAY FLUX x COS X erg x10⁻³/cm² sec
22
18
14
10
6
2
NOV.
JAN.
FEB.
WEEKS
3.5
3.3
3.1
2.9
FoE mc/sec (OTTAWA 1200 hrs.)

FIGURE-4

FoE mc/sec (OTTAWA 1200 hrs)
3.4
3.3
3.2
3.1
3.0
2.9
WEEKS
FEB
JAN
NOV
3
2
1
44-60 Å XRAY FLUX x COS X ERG x 10⁻¹/CM² SEC

FIGURE-5

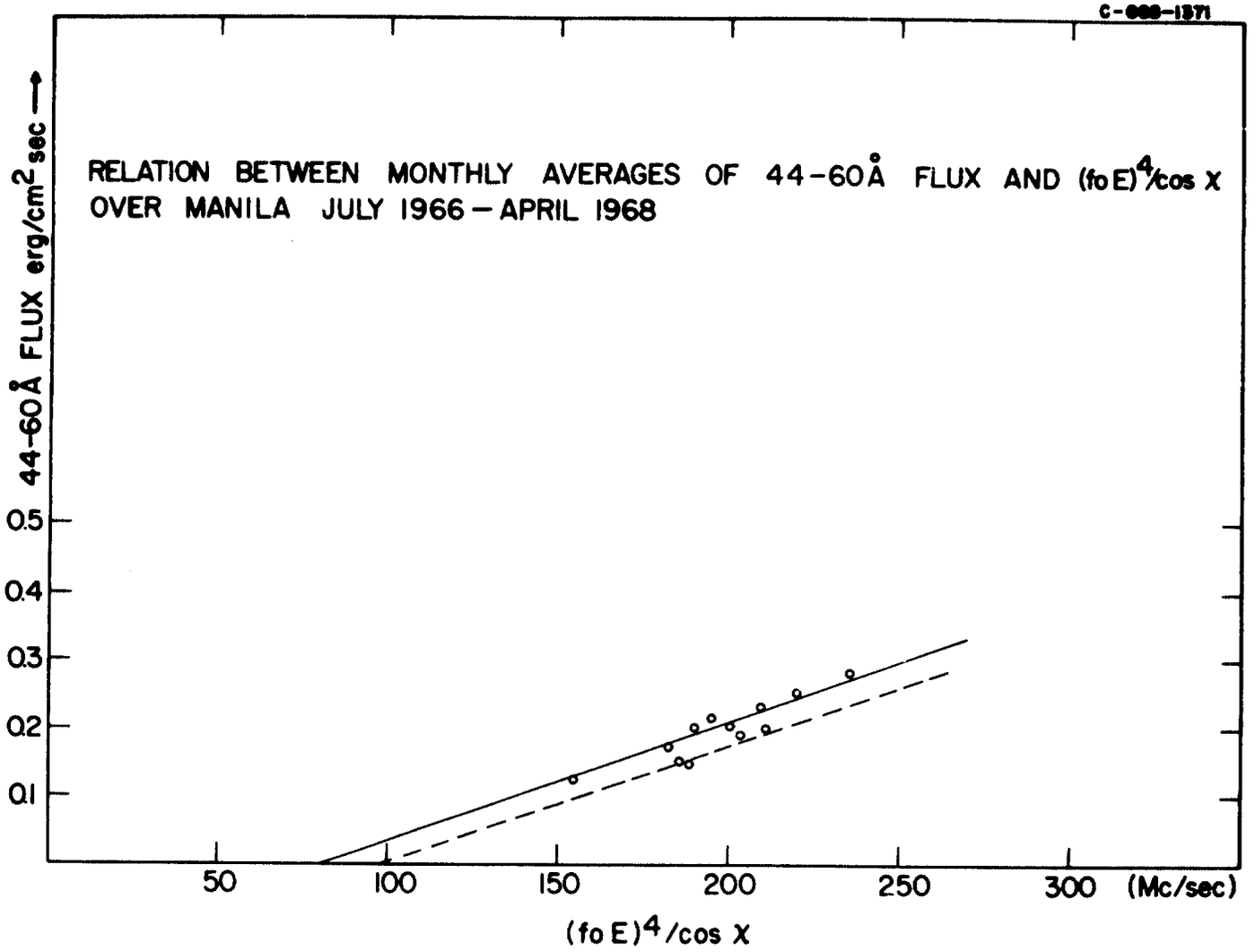
C-888-1371
RELATION BETWEEN MONTHLY AVERAGES OF 44-60Å FLUX AND (foE)4/cos X
OVER MANILA JULY 1966 – APRIL 1968
44-60Å FLUX erg/cm2sec
0.5
0.4
0.3
0.2
0.1
50
100
150
200
250
300
(Mc/sec)
(foE)4/cos X

FIGURE 6

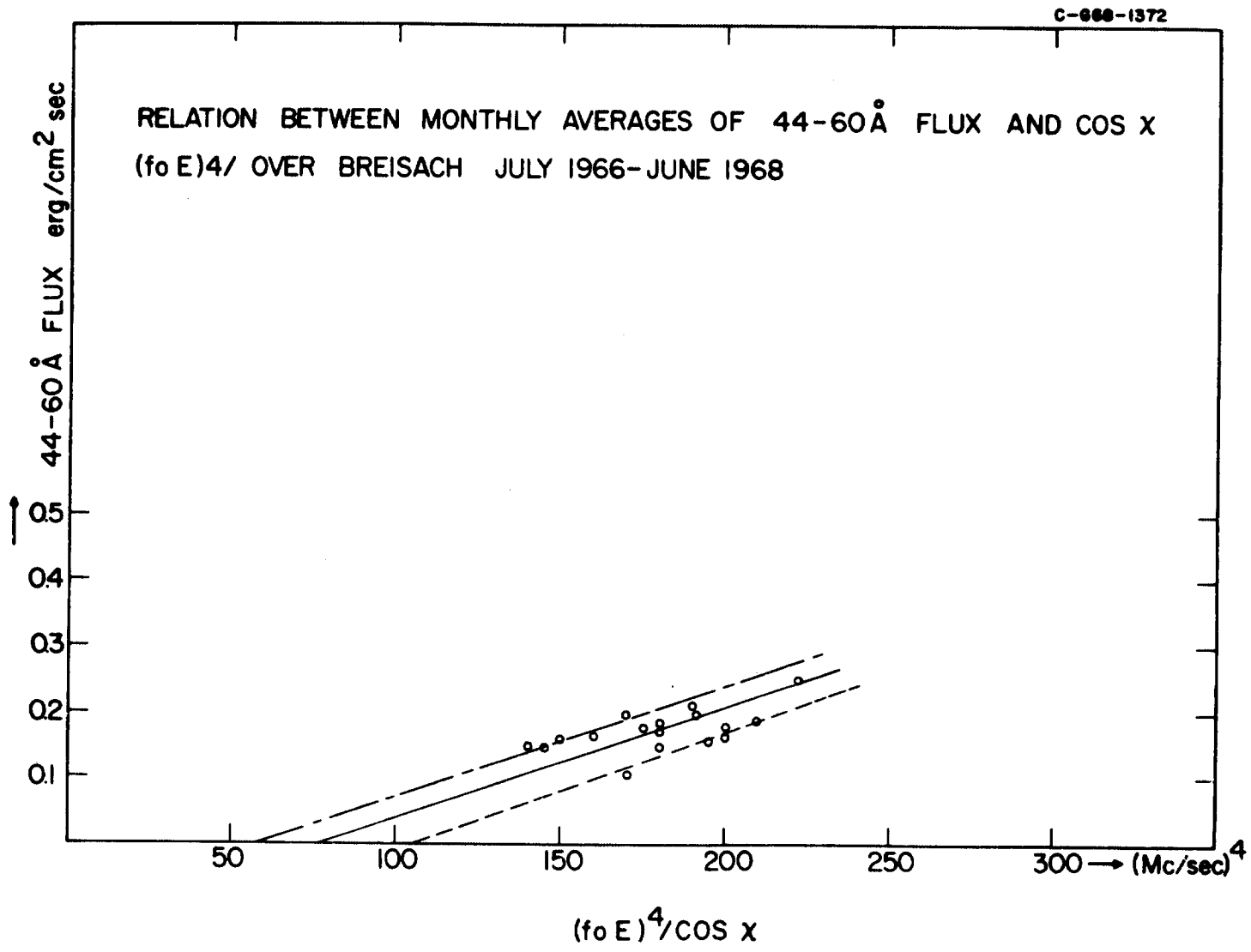
C-668-1372
RELATION BETWEEN MONTHLY AVERAGES OF 44-60Å FLUX AND COS X
(fo E)4/ OVER BREISACH JULY 1966-JUNE 1968
44-60 Å FLUX erg/cm2 sec
0.5
0.4
0.3
0.2
0.1
50
100
150
200
250
300 → (Mc/sec)4
(fo E)4/COS X

FIGURE 7

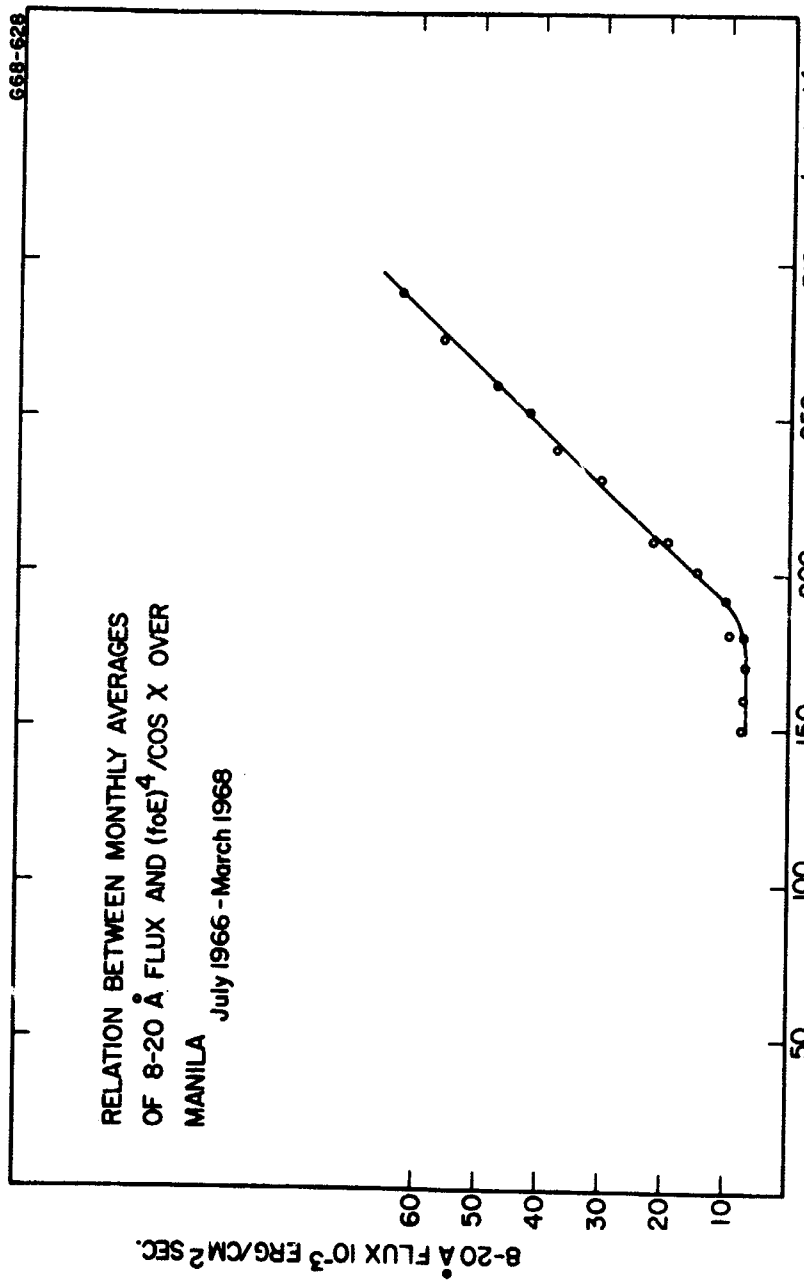
668-628
RELATION BETWEEN MONTHLY AVERAGES
OF 8-20 Å FLUX AND (foE)^4/COS X OVER
MANILA
July 1966 - March 1968
8-20 Å FLUX 10^{-3} ERG/CM^2 SEC.
10
20
30
40
50
60
50
100
150
200
250
310
(mc/sec)4
(foE)^4/COS X

FIGURE-8

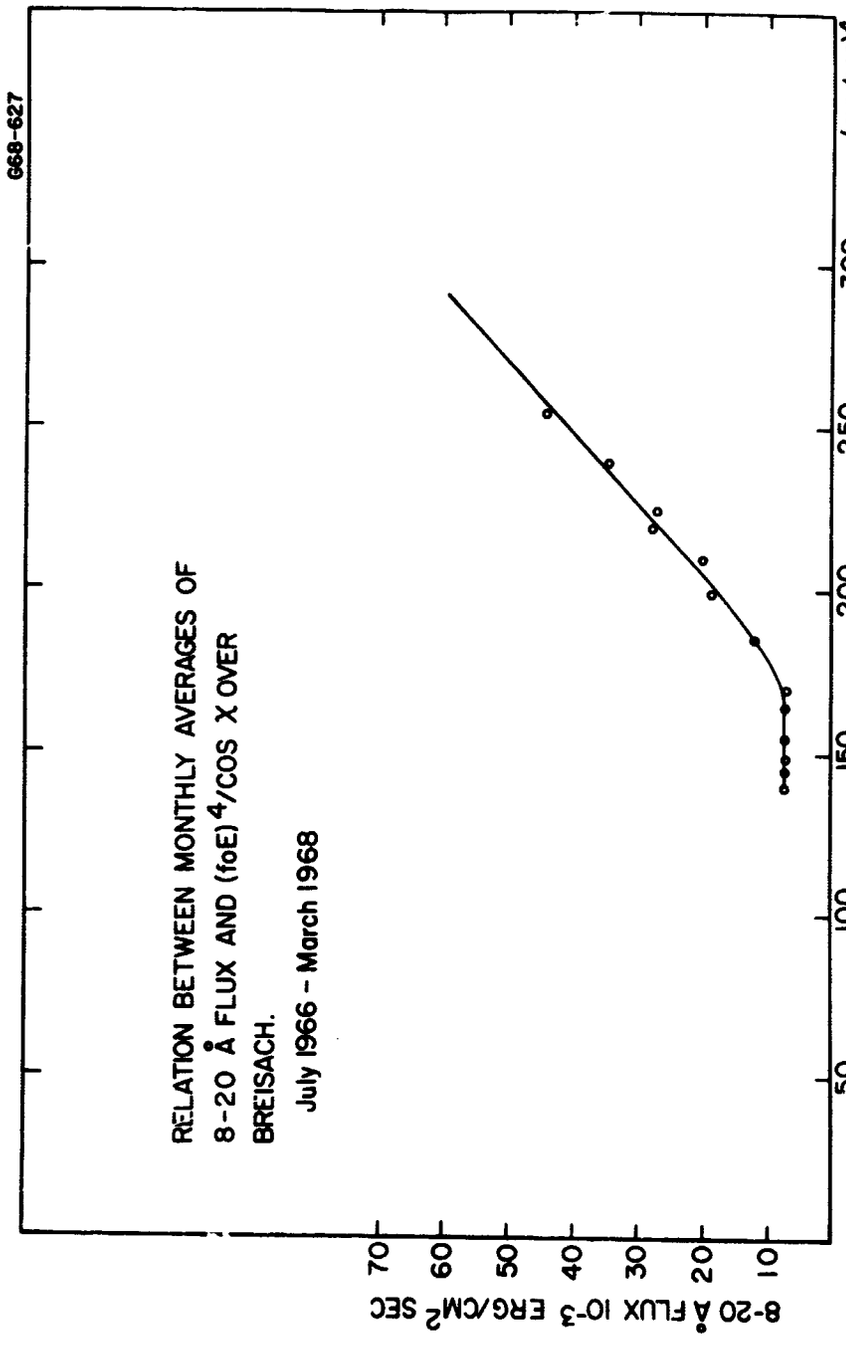
G68-627
RELATION BETWEEN MONTHLY AVERAGES OF
8-20 Å FLUX AND (foE)4/COS X OVER
BREISACH.
July 1966 - March 1968
8-20 Å FLUX 10-3 ERG/CM2 SEC
10
20
30
40
50
60
70
50
100
150
200
250
300
(mc/sec)4
(foE)4/COS X

FIGURE-9

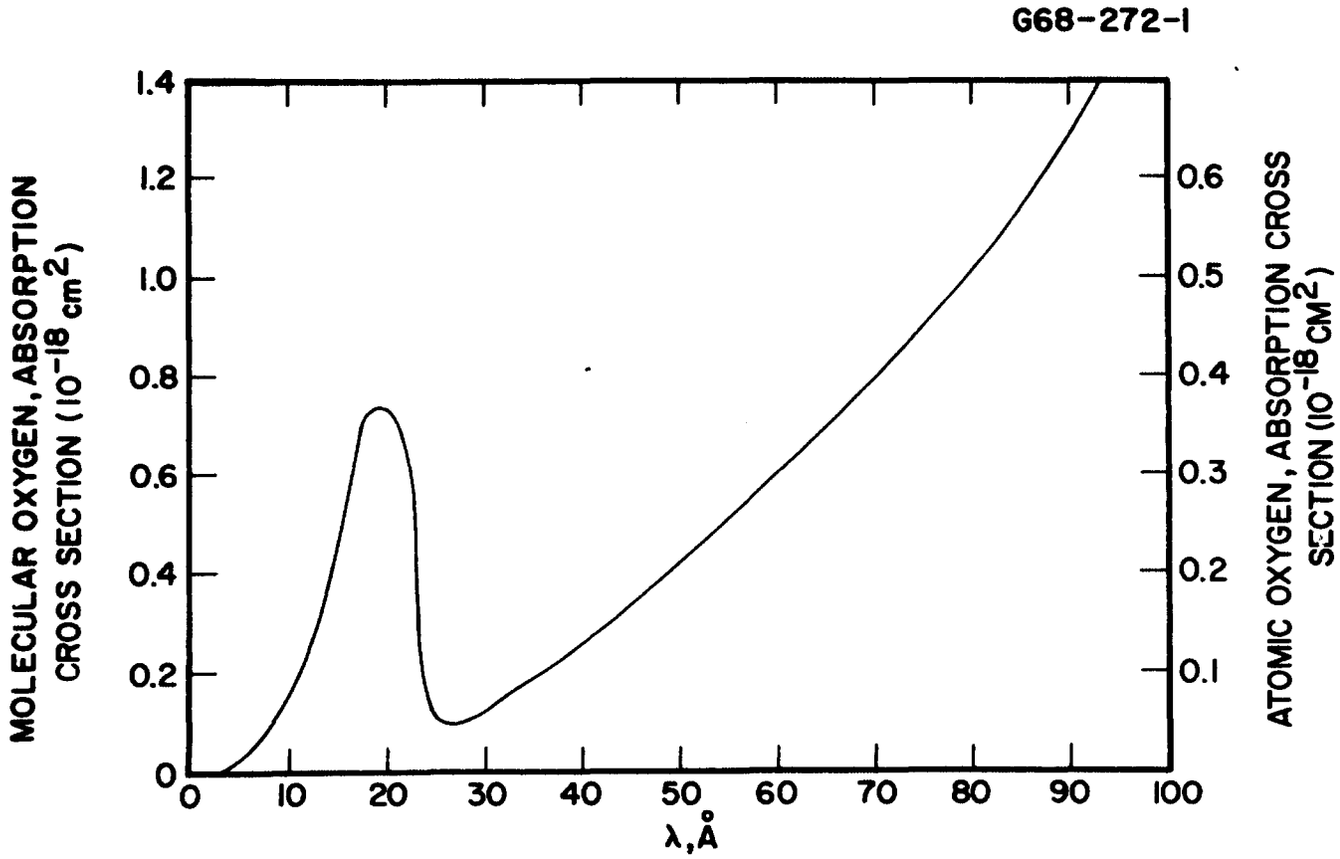

FIG. 10 ABSORPTION CROSS SECTIONS FOR OXYGEN.

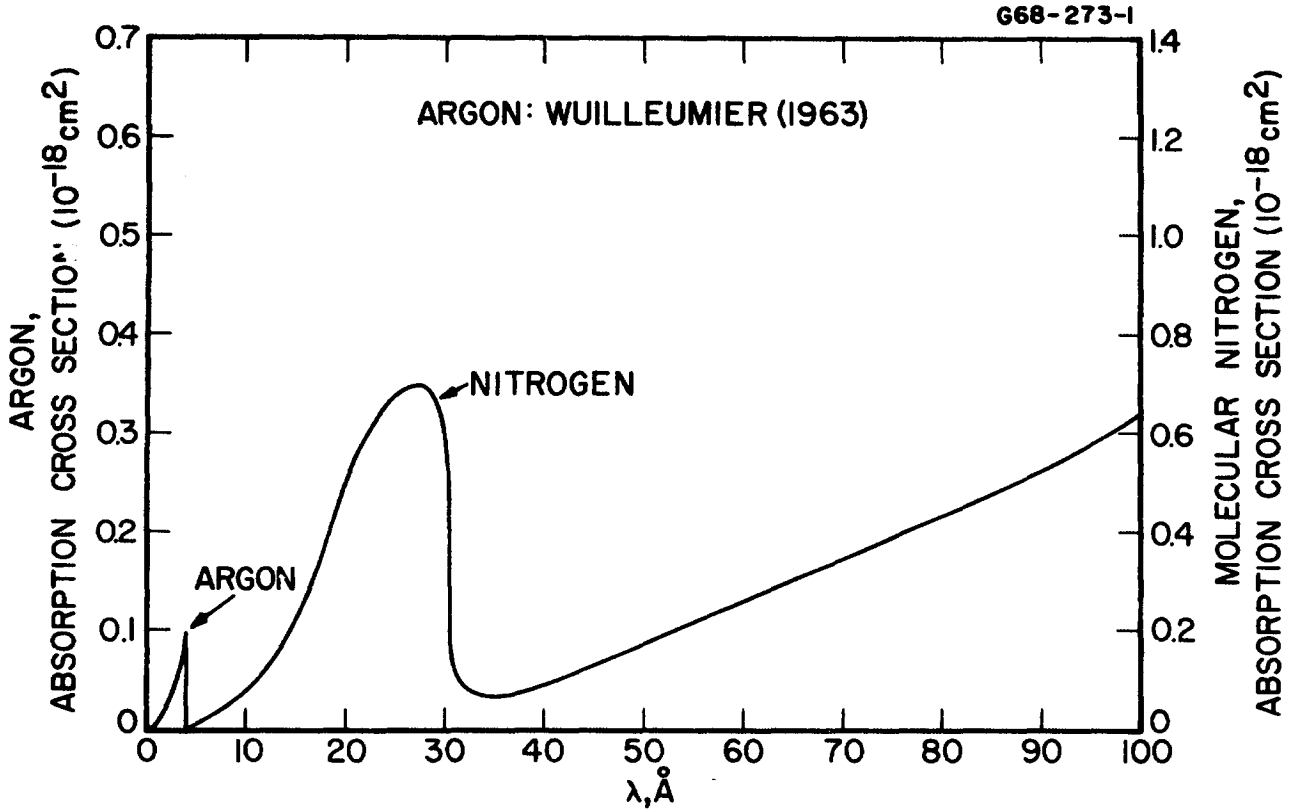

FIG. 11 ABSORPTION CROSS SECTIONS FOR MOLECULAR NITROGEN AND FOR ARGON.

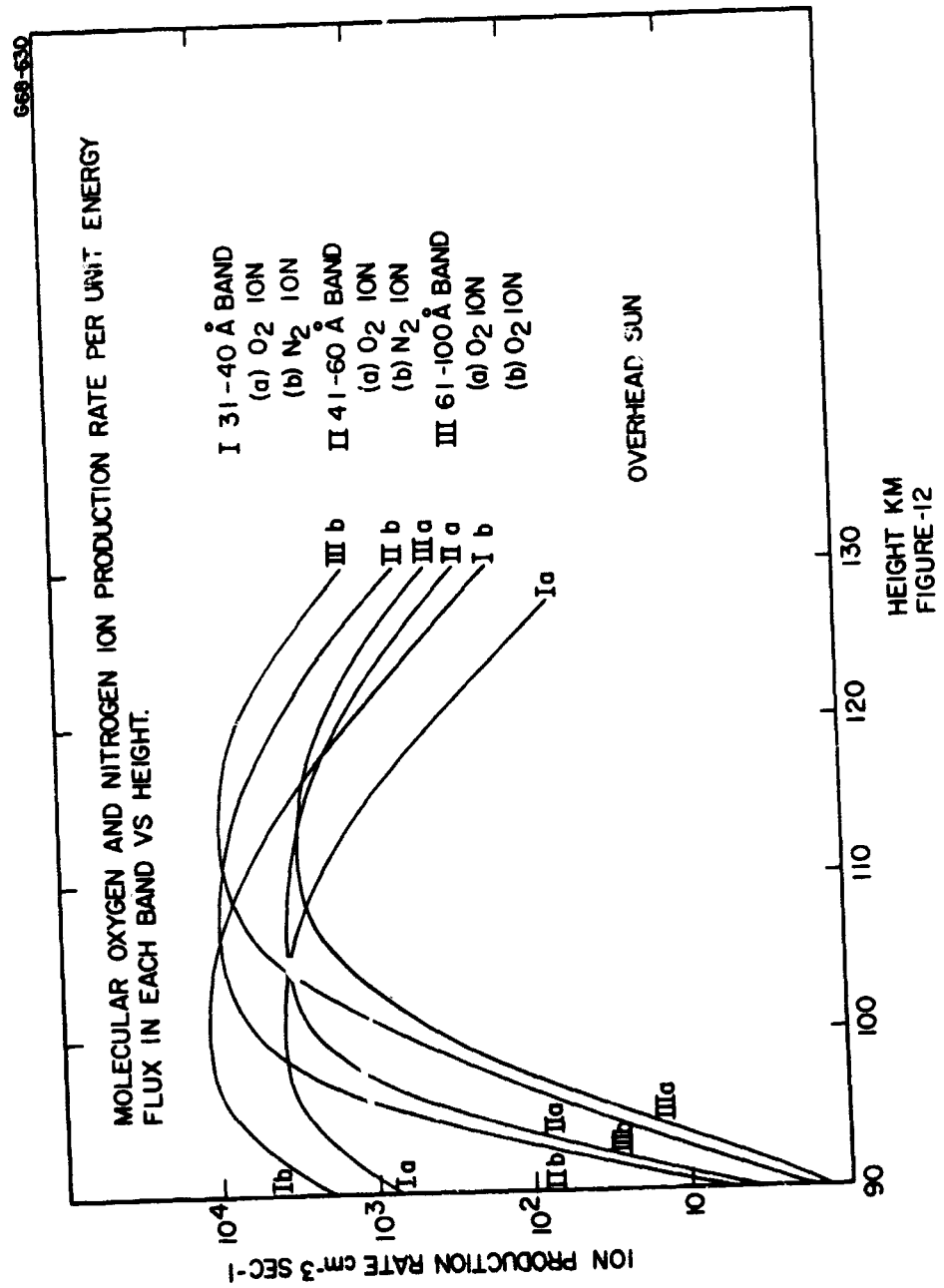
MOLECULAR OXYGEN AND NITROGEN ION PRODUCTION RATE PER UNIT ENERGY FLUX IN EACH BAND VS HEIGHT.
I 31-40 Å BAND
(a) O2 ION
(b) N2 ION
II 41-60 Å BAND
(a) O2 ION
(b) N2 ION
III 61-100 Å BAND
(a) O2 ION
(b) O2 ION
OVERHEAD SUN
ION PRODUCTION RATE cm-3 SEC-1
HEIGHT KM

FIGURE-12

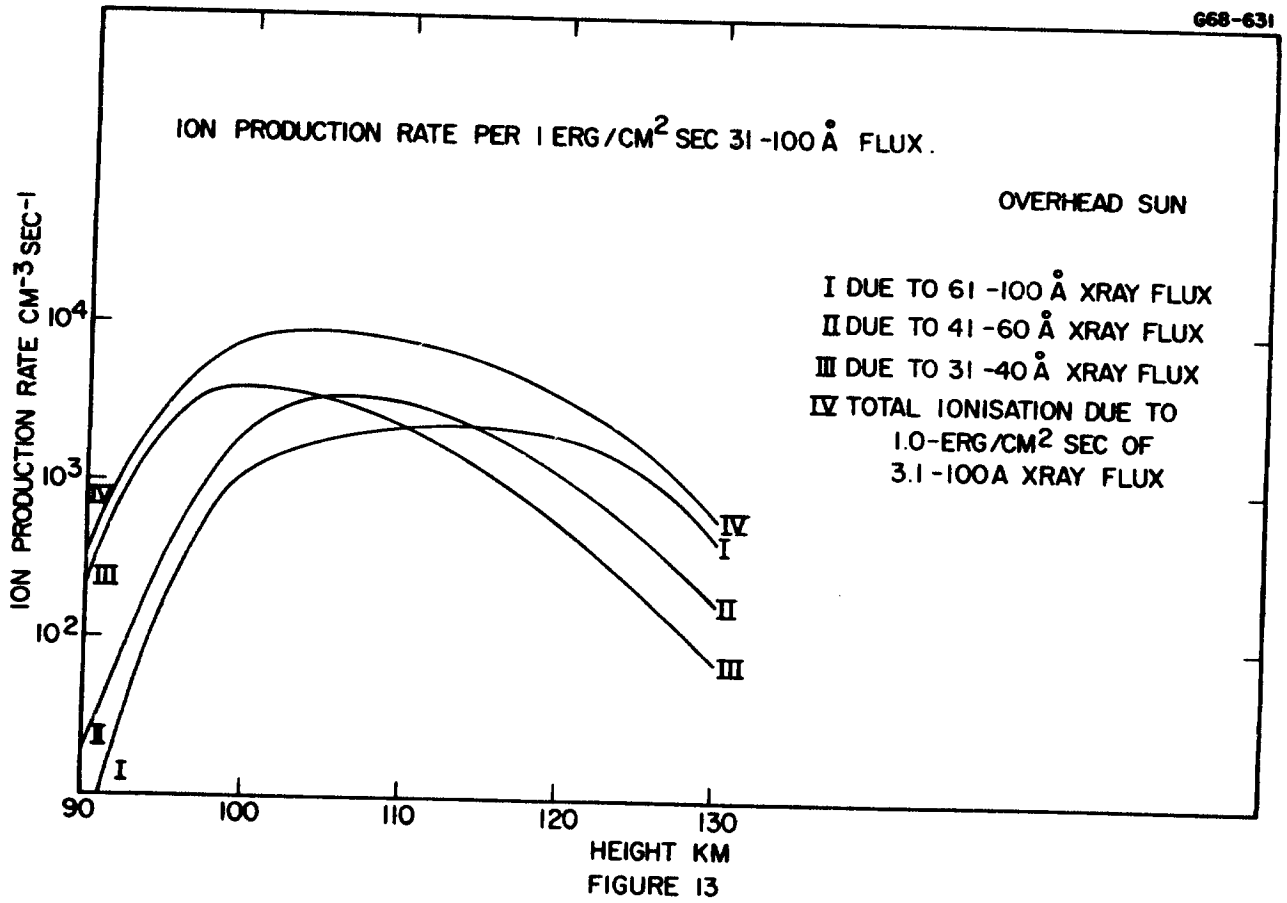
G68-631
ION PRODUCTION RATE PER 1 ERG/CM^2 SEC 31-100 Å FLUX.
OVERHEAD SUN
I DUE TO 61-100 Å XRAY FLUX
II DUE TO 41-60 Å XRAY FLUX
III DUE TO 31-40 Å XRAY FLUX
IV TOTAL IONISATION DUE TO 1.0-ERG/CM^2 SEC OF 3.1-100A XRAY FLUX
ION PRODUCTION RATE CM^{-3} SEC^{-1}
10^4
10^3
10^2
90
100
110
120
130
HEIGHT KM

FIGURE 13

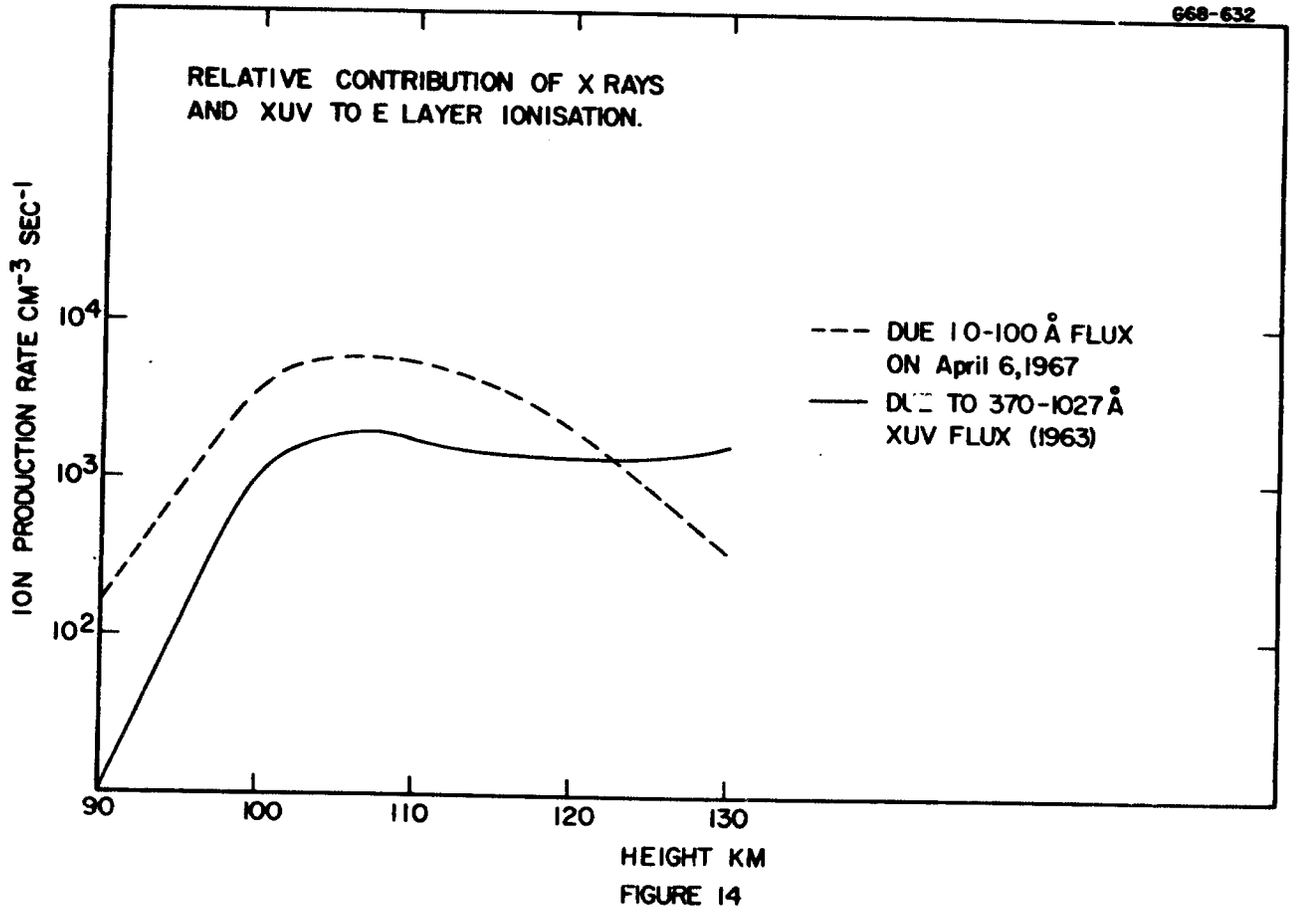
668-632
RELATIVE CONTRIBUTION OF X RAYS
AND XUV TO E LAYER IONISATION.
ION PRODUCTION RATE CM-3 SEC-1
10^4
10^3
10^2
90
100
110
120
130
HEIGHT KM
--- DUE 10-100 Å FLUX
ON April 6,1967
—— DUE TO 370-1027 Å
XUV FLUX (1963)

FIGURE 14

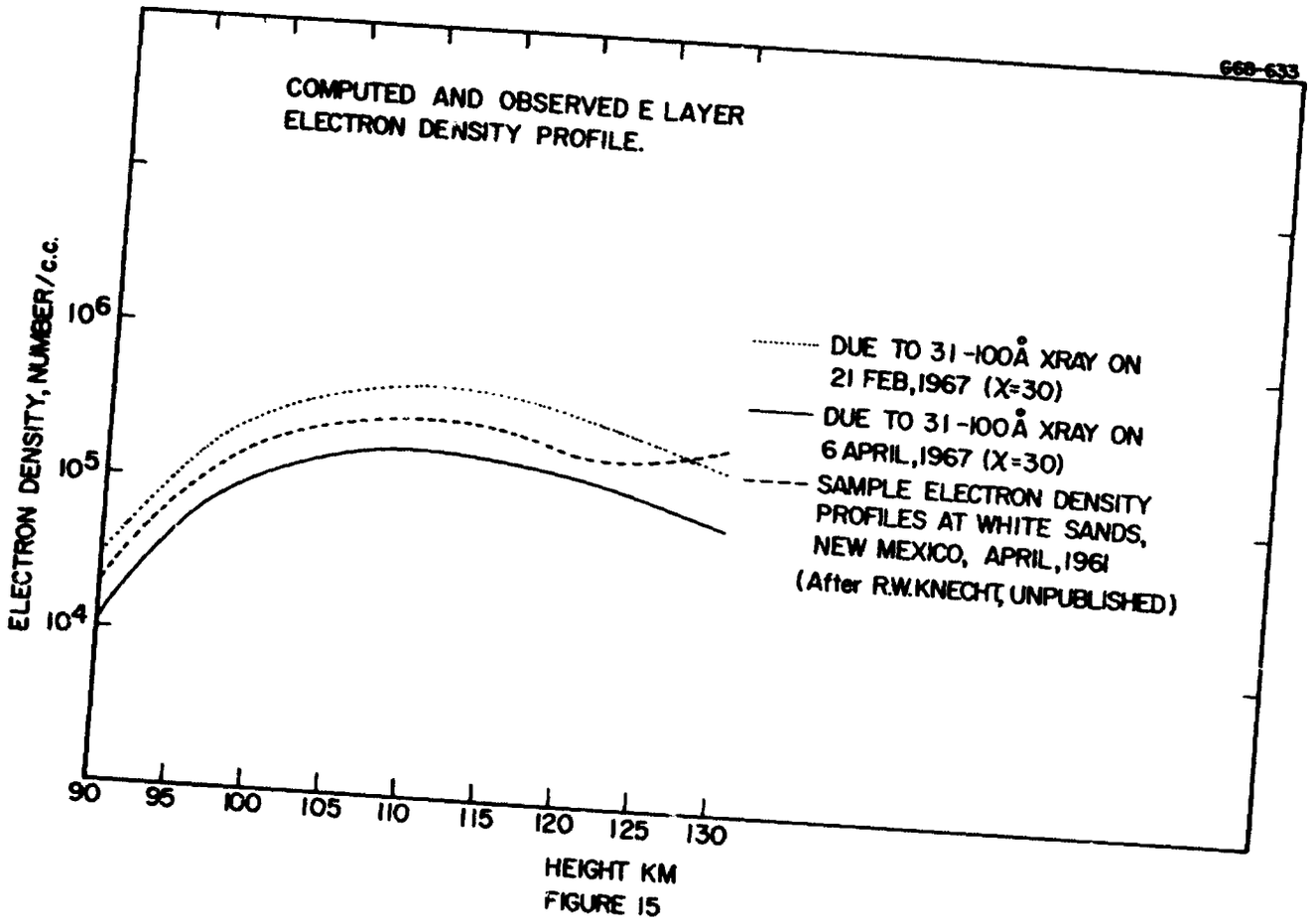
COMPUTED AND OBSERVED E LAYER
ELECTRON DENSITY PROFILE.
668-633
ELECTRON DENSITY, NUMBER/c.c.
10^6
10^5
10^4
DUE TO 31-100Å XRAY ON 21 FEB, 1967 (X=30)
DUE TO 31-100Å XRAY ON 6 APRIL, 1967 (X=30)
SAMPLE ELECTRON DENSITY PROFILES AT WHITE SANDS, NEW MEXICO, APRIL, 1961
(After R.W. KNECHT, UNPUBLISHED)
90
95
100
105
110
115
120
125
130
HEIGHT KM

FIGURE 15

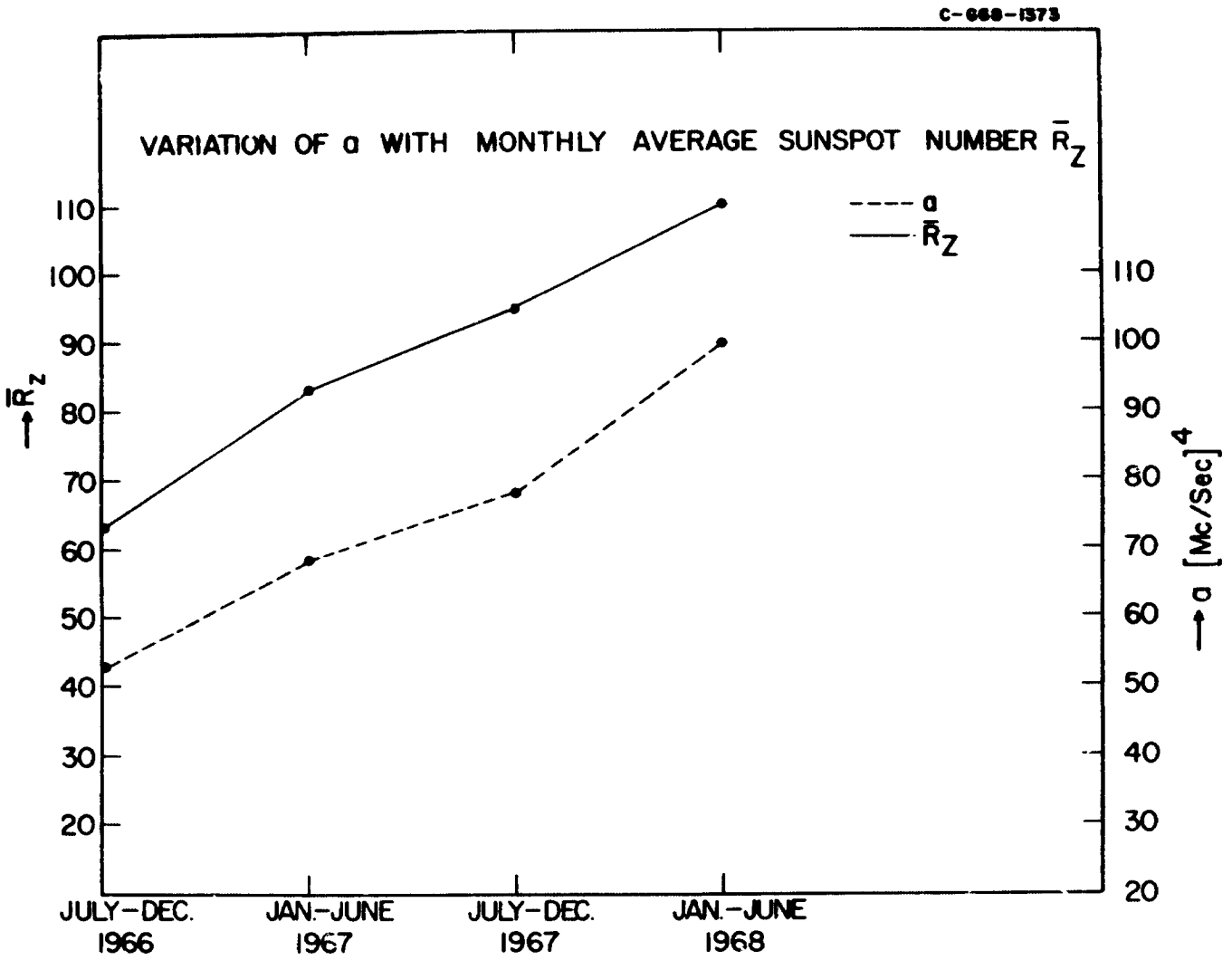
C-668-1373
VARIATION OF a WITH MONTHLY AVERAGE SUNSPOT NUMBER $\bar{R}_Z$
a
$\bar{R}_Z$
110
100
90
80
70
60
50
40
30
20
$\bar{R}_Z$
a [Mc/Sec]^4
JULY–DEC. 1966
JAN.–JUNE 1967
JULY–DEC. 1967
JAN.–JUNE 1968

FIGURE 16